Journal of
Stem Cell Reports

JScholar
Fostering Scholarly Communication

Research Open Access

A New Ball for an Old Trick: Paramagnetic Cell Sorting of Human Mesenchymal Stem Cells from Adipose Tissue

John D. Murray MD, FACS[1,*], Andria Doty, PhD[2], Noah Jones, BS[3], Marie Crandall, MD, MPH, FACS[4], Edward W. Scott, PhD[5]

[1]University of Florida at Jacksonville, Division of Plastic Surgery, The Regenerative Medicine Laboratory Jacksonville, FL, USA
[2]University of Florida at Gainesville, Interdisciplinary Center for Biotechnology Research, Gainesville, FL, USA
[3]University of Florida at Gainesville, Interdisciplinary Center for Biotechnology Research, Gainesville, FL, USA
[4]University of Florida at Jacksonville, Department of Surgery, Jacksonville, FL, USA
[5]University of Florida at Gainesville, Department of Microbiology and Molecular Genetics, Gainesville, FL, USA

***Corresponding author:** John Murray, MD, FACS, 653 West 8th Street, Faculty Bldg., 3rd floor, Jacksonville, FL 32209, 904-244-3915, Fax 904-244-3870; Email: john.murray@jax.ufl.edu

Received Date: August 12, 2019 **Accepted Date:** September 09, 2019 **Published Date:** September 11, 2019

Citation: John D. Murray (2019) A New Ball for an Old Trick: Paramagnetic Cell Sorting of Human Mesenchymal Stem Cells from Adipose Tissue. J Stem Cell Rep. 1: 1-11.

Abstract

Adipose tissue-derived mesenchymal stem cells (ASCs) may be isolated in clinically useful quantities without *in vitro* expansion. The purpose of this study is to validate a novel method for the enrichment of primary ASCs using paramagnetic beads. Primary rabbit anti-mouse antibodies were bound to paramagnetic microbeads. Secondary antibodies, selective for ASCs, were then bound to the primary antibodies to construct so-called paramagnetic immunobeads (PIBs). PIBs were then added to fresh human lipoaspirate to create ASC-PIB conjugates (aPIBS) over 10 minutes. A hand-held magnet was then placed adjacent to the lipoaspirate-aPIBs mixture, and over the next 10 minutes, the aPIBs were precipitated. Live cell count per mL of lipoaspirate was 9.6 x 10^4. Scanning electron microscopy revealed precipitates consistent with aPIBs. Flow cytometry identified cell-bound markers for CD90 and CD105 while culture confirmed tri-lineage differentiation, all attributes diagnostic of ASCs. This study validates that functional ASCs may be isolated from lipoaspirate by magnetic enrichment in 20 minutes. As both the harvest of adipose tissue by liposuction and this ASC enrichment technique do not require electricity, fresh primary therapeutic ASCs may be isolated in any point-of-care setting, even in developing countries.

Keywords: Mesenchymal stem cells; adipose-derived stem cells; hematopoietic stem cells; point-of-care systems; single-use systems; regenerative medicine.

Abbreviations: HSCs= hematopoietic stem cells; MSCs= mesenchymal stem cells; BMSCs= bone marrow-derived mesenchymal stem cells; ASCs= adipose-derived mesenchymal stem cells; PCS=paramagnetic cell sorting; PIB= paramagnetic immunobead; aPIB= ASC-paramagnetic bead conjugate

Introduction

Hematopoietic stem cells (HSCs) and mesenchymal stem cells (MSCs), the only known naturally occurring types of adult human stem cells, exhibit similar qualities. Both are essential to life, both reside in bone marrow [1,2], and both provide necessary multi-lineage regenerative capabilities: hematopoietic stem cells (HSCs) regenerate cells of the blood [3-5] and mesenchymal stem cells (MSCs) regenerate cells of solid tissues [6]. While bone marrow remains a common source for both therapeutic HSCs and MSCs [7], MSCs also reside in solid tissues, to include adipose tissue (these cells being termed adipose-derived stem cells, ASCs) [8]. ASCs exhibit similar qualities to bone marrow-derived stem cells [8,9]. However, it has been reported that, per equal volume, adipose tissue yields considerably more, often quoted as hundreds of folds more, MSCs than bone marrow [10-13]. One study concluded that 1 gm of aspirated adipose tissue yields approximately 3.5 x 10^5 to 1 x 10^6 ASCs compared to 500 to 5 x 10^4 of bone-marrow derived MSCs (BMSCs) isolated from 1gm of bone marrow aspirate [14]. Additionally, ASCs may be isolated in clinically useful quantities without *in vitro* expansion, as many therapies using BMSCs require due to smaller primary quantities respectively [15]. As the field of clinical regenerative medicine and tissue engineering using MSCs continues to rapidly grow, MSC isolation techniques that are more efficient, simplified, and ready-to-use are needed.

Much of the current methodology regarding adult stem cell isolation comes from over 60 years of hematopoietic bone marrow transplantation. HSCs were historically harvested directly from bone marrow, commonly from the iliac bone. However, to increase yield and decrease morbidity, HSCs are now more commonly harvested from peripheral blood through apheresis after the HSCs have been mobilized from the marrow to the circulating peripheral system [16] Apheresis relies on centrifugation separation principles to isolate white blood cells and then returns the red blood cells to the donor. As such, only 5 to 20 % of the collected cells are true HSCs; other constituents include progenitor cells and white blood cells in varying stages of maturity [17]. Methods to purify the collected white cell subpopulation then relies on techniques based on physical parameters (cell size and density) or techniques based on affinity (chemical, electrical, or magnetic couplings) [18]. Examples of purifying techniques based on physical parameters include density gradient centrifugation, field flow fractionation, and dielectrophoresis [18]. Separation methods based on physical parameters lack the ability to highly purify the stem cell target population as the size and density differences between stem cell and non-stem cells are not absolute [18]. Affinity-based separation methods include fluorescence-activated cell sorting, which can provide a highly pure (95% or higher) cell population, or magnet activated cell sorting, which provides stem cell purities of at least 75% [19,20]. FACS requires bulky expensive equipment and has limited throughput (about 10^7 cells/hour) while magnetic activated cell sorting allows target cell processing in parallel, achieving faster separation (about 10^{11} cells/hour) [16, 21, 22].

Paramagnetic beads have shown great utility in paramagnetic cell sorting (PCS) of HSCs since their initial discovery in 1977 [23-26]. These beads are spherical polymer-coated ferrous particles of uniform size. As paramagnetic, the beads move toward magnetic forces, though they do not retain any significant magnetism once the magnetic force is removed. Their surface allows attachment of bioreactive molecules, such as antigens and antibodies, for the immunoprecipitation of cells, proteins, and DNA. Paramagnetic beads are commercially available in primarily two different sizes: as nanoparticles (typically 50-300 nm) or as microspheres (1-5 μm) [27]. The performance of PCS for the enrichment of HSCs commonly uses nanoparticles as theyare efficacious in fluids and do not have to be unconjugated from the HSCs for subsequent flow cytometric analysis [28]. Microspheres, as conjugated to their target cells, can interfere with flow cytometry due to their greater mass and auto-fluorescence.

Three key points regarding magnetic force on a particle need to be recognized. First, the magnetic force on a particle is proportional to the particle's diameter cubed, thus moving very small paramagnetic nanoparticles is more difficult than the larger microspheres [29]. Second, assuming that the particle has reached its saturation magnetization, the magnetic force is proportional to the magnetic field gradient and not the magnetic field strength [29]. Third, a particle moving through a fluid encounters a drag force proportional to its velocity relative to the fluid. Thus, the higher the drag force, the higher the magnetic field gradient needed to counteract the drag force [29]. For cell enrichment purposes, using paramagnetic nanoparticles in high drag force environments, such as tissues (versus low drag hematopoietic fluid environments), requires high-gradient magnetism, typically generated from electro magnetics. However, as microspheres are considerably larger and thus portend a higher magnetic force, we theorize that bar magnets may create a high enough magnetic force and magnetic field gradient to separate ASCs from previously aspirated adipose tissue.

The purpose of this study is to validate a novel method, a method based on magnetic enrichment of therapeutic hematopoietic stem cells, for the enrichment of primary ASCs using

paramagnetic microspheres and a hand-held bar magnet.

Methods

Lipoaspirate harvest

Fresh human lipoaspirate obtained from informed and consented healthy females was used for this study (University of Florida Jacksonville Institutional Review Board approved study, IRB# 201601520). The lipoaspirate had been harvested using standard operative tumescent techniques using syringe liposuction. The tumescent solution included normal saline, lidocaine, and epinephrine. Shortly after harvest, the fresh lipoaspirate underwent 20 intersyringe transfers (10 mls syringes). After separating into principally aqueous and adipose layers, the aqueous layer was decanted. The remaining adipose layers were combined for a total working volume of 15 mls. This study incorporated triple biological replicates with double technical replicate testing for cell quantity (average taken) and electron microscopy.

ASC isolation by paramagnetic immunoprecipitation

ASC-paramagnetic immunobead (aPIB) preparation

aPIBs were prepared to recognize a panel of ASC cell surface markers (CD90, CD44, CD105, and CD73) using the Dynabeads® protein G immunoprecipitation kit (Thermo Fisher Scientific, Waltham, MA, cat#10007D) according to the manufacturer's instructions. Briefly, 50 µL of the Dynabeads® were conjugated to protein G in a microfuge tube. A neodymium magnet (3x0.2x0.5 inch, Omega Magnets, Carpinteria, CA) was then placed next to the tube to precipitate the beads and the supernatant was removed. To the bead suspension, 200 µL of antibody binding and washing buffer and 5µL of rabbit anti-mouse IgG antibody (Thermo Fisher Scientific, cat# A27022) were added. The suspension was then rotated (360° rotation, HulaMixer®, Thermo Fisher Scientific, cat#15920D) for 10 minutes at room temperature. The beads were then precipitated once again with the magnet and the supernatant was removed and 200 µL of the washing buffer was added. Then, 5 µL each of mouse anti-human IgG antibodies of markers CD90, CD44, CD105, and CD73 (BD Biosciences, Franklin Lakes, NJ, cat#562245), suitable for ASC enrichment, were added to the tube and incubated in similar rotation for 10 minutes. The supernatant was removed after magnetic immunoprecipitation and 200 µL of the washing buffer was added and the programmed paramagnetic beads, now aPIBs, were then briefly vortexed to homogeneous suspension. A structural aPIB diagram is seen in (figure 1).

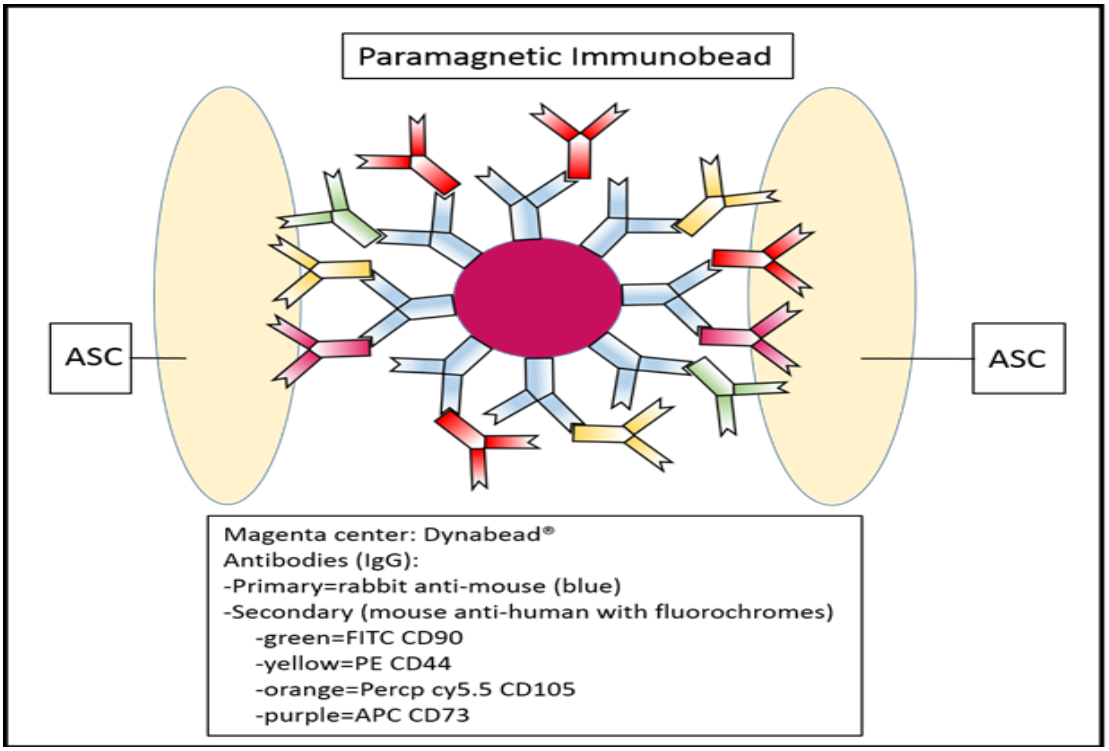

Figure 1. Paramagnetic immunobead.

Primary and secondary IgG antibodies, diagnostic of ASCs, are built onto a paramagnetic microbead, creating a paramagnetic immunobead. Layering the antibodies respectively may reduce steric hindrance and improve binding strength to conjugated ASCs.

aPIB immunoprecipitation

The 15 mls of lipoaspirate was added to an empty 15 mL polypropylene coned tube and the 200 µL suspension of PIBs was added to the tube. The tube was capped and then held and rotated in hand for 10 minutes. With the tube returned to the upright position, the magnet was then placed parallel and adjacent to the long axis of the tube. Over the next 10 minutes, the magnet was steadily moved toward the coned bottom of the tube to precipitate the aPIBs to the bottom of the coned tube (see figure 2). The lipoaspirate was then discarded and the aPIBs were resuspended in 1mL of Dulbecco's phosphate buffered saline (STEMCELL Technologies, cat#37350) for subsequent cell counting and culture. No attempt to unconjugate the PIBs from the ASCs was made.

aPIB cell counting

10 µL samples from the aPIB suspension then underwent automated cell counting and trypan blue viability testing in accordance with the manufacturer's instructions (Countess™ II, Thermo Fisher Scientific, cat#AMQAX1000). Final count was the average of two counts respectively.

aPIB morphologic evaluation

aPIBs underwent morphologic evaluation using scanning electron microscopy (SEM).

aPIB suspensions were gently filtered onto poly-L-lysine treated 0.2um Millipore filters and fixed with 2.5% glutaraldehyde, 4% paraformaldehyde in 1xPBS, pH 7.24. Filters with aPIBs were washed with 1XPBS followed by deionized water and dehydrated in a graded ethanol series (25%, 50%, 75%, 95%, and 100%). Dehydrated cells were then loaded into the critical point dryer with bone dry CO_2 (Autosamdri-815, Tousimis, Rockville, MA). Dried membrane filters containing aPIBs were mounted onto aluminum stubs with carbon adhesive tabs, sputter coated with Au/Pd (DeskV, Denton, Moorestown, NJ) and imaged with Hitachi SU5000 FE-SEM (Hitachi High Technologies, Schaumburg, IL).

aPIB immunophenotyping

Samples of the aPIB suspension were run on a BD LSR II (BD Biosciences, San Jose, CA) flow cytometer with accompanying analytical software (BD FACSDiva™). The aPIBs were suspended in BD Pharmingen™ Stain Buffer (cat#554656). In accordance with the Becton-Dickenson Stemflow™ kit, 100 µl of the prepared suspension was added equally to all analysis tubes to include FITC mouse anti-human CD90, PE mouse anti-human CD44, PerCP-Cy™5.5 mouse anti-human CD105, and APC mouse anti-human CD73 with positive and negative controls and positive and negative cocktails. After the cell suspensions were added, the tubes were incubated in the dark for 30 minutes and the cells were then washed twice with BD Pharmingen™

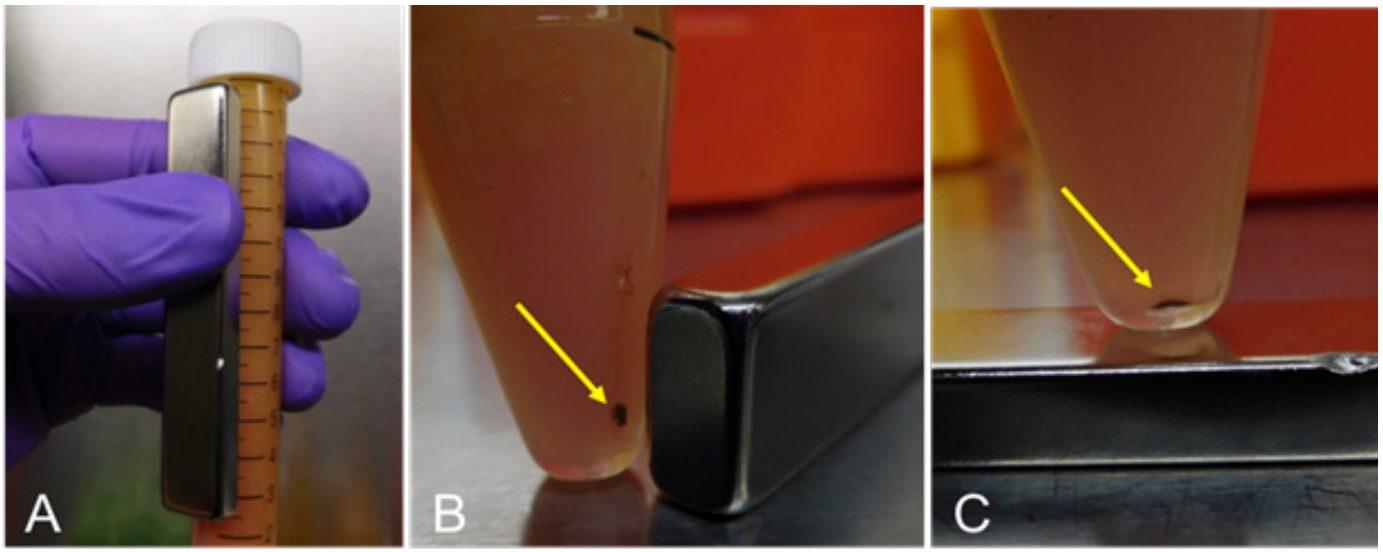

Figure 2. Paramagnetic immunoprecipitation of ascs.

After placement of the paramagnetic immunobeads (PIBs) into the lipoaspirate, the tube containing the lipoaspirate-PIB mixture is manually held and rotated for 10 minutes. Over the next 10 minutes, a neodymium bar magnet is moved from alongside the tube to the bottom of the tube (panels A-C) to precipitate the ASC-PIBs conjugates (arrows). The lipoaspirate is then simply discarded.

Stain Buffer and resuspended to 500 µl in BD Pharmingen™ Stain Buffer. Cells were then kept in the dark and on ice until analysis later that same day.

ASC functional analysis by differentiation

ASC expansion

The aPIBs were added to 5 mls of animal component free defined media (MesenCult-ACF basal medium #05451 and 5X supplement #05452, STEMCELL Technologies, Vancouver, BC) into a T-25 culture flask (pre-treated with attachment substrate, STEMCELL Technologies, #05444. Flask: VWR, Nunclon tissue culture flask #470174-450) and incubated at humidified 5% carbon dioxide. Half media change was performed at day 6 with complete media change at day 10. Observation of ASC adherence and morphology were completed and recorded around culture day 14.

Tri-lineage differentiation to confirm ASC enrichment

Expanded cells at initial 80% confluence (typically culture day 6 or 7) were dissociated from the culture flask (Mesencult-ACF Dissociation Kit #05426, Stemcell™ Technologies). ASCs were first passaged and seeded on six-well culture plates at approximately 100,000 cells per well. After attachment, cells were grown to approximately 80% confluence. Each well received a different respective differentiation medium.

For osteogenic differentiation, basal growth media was exchanged for conditioned osteogenic differentiation medium (Stemcell™ Technologies, Mesencult™ Osteogenic Stimulatory Kit #05404). Alizarin Red (Sigma-Aldrich, St. Louis, MO) staining was performed (to specifically stain alkaline phosphatase deposits) on day 14 and photomicrographs were obtained using whole field bright-light microscopy captured at 20x.

For adipogenic differentiation, basal growth media was exchanged for conditioned adipogenic differentiation medium (Stemcell™ Technologies, Mesencult™ Adipogenic Differentiation Medium #05412). Oil red O (Sigma-Aldrich) staining was performed (to specifically stain the lipid droplets) on day 14 and microphotographs were obtained using whole field bright-light microscopy captured at 10x.

For chondrogenic differentiation, basal growth media was exchanged for conditioned chondrogenic differentiation medium (Stemcell™ Technologies, Mesencult™ Chondrogenic Differentiation Medium #05455). Alcian Blue / Nuclear Fast Red (Sigma-Aldrich) staining was performed (to specifically stain sulfated proteoglycans) on day 14 and photomicrographs were obtained. The micromass chondrosphere was photographed by indirect microscopy.

Results

aPIB cell counting

Live cell count per mL lipoaspirate processed was 9.6 x 10^4.

aPIB morphologic evaluation

Our initial goal was to ensure that the aPIB based ASC enrichment protocol was directly isolating cells with an ASC morphologic phenotype. Therefore, we performed scanning electron microscopy (SEM) of the aPIB isolates (see figure 3). While cells phenotypically consistent with erythrocytes and lymphocytes were seen, the PIBs were only attached to cells morphologically consistent with ASCs. This visually confirmed that the direct isolation protocol enriches for cells with the expected ASC phenotype, not random cell precipitation. We suspect that processing of the samples for SEM unconjugated many of the PIBs from ASCs.

aPIB immunophenotyping

Immunophenotyping by flow cytometry confirmed cells positive for markers CD90 and CD105 (see figure 4). While the fluorochromes of FITC (CD90) and PerCP-Cy™5.5 (CD105) were clearly displayed, the auto-fluorescence of the Dynabeads® masked the fluorescence of APC (CD73) and PE (CD44). While the flow of the aPIB suspension through the aspiration nozzle did slow from time to time, dilution of the sample with stain buffer helped to re-establish faster flows.

ASC functional analysis by differentiation

The ASCs underwent plastic adherence, colony formation, and sphere formation, phenotypically diagnostic of adipose-derived stem cells (see figure 5). Differentiation to chondroblasts, osteoblasts, and adipocytes was confirmed by appropriate lineage staining. By culture day 10, the ASC 2-dimensional monolayer had developed into spheroids (see figure 6).

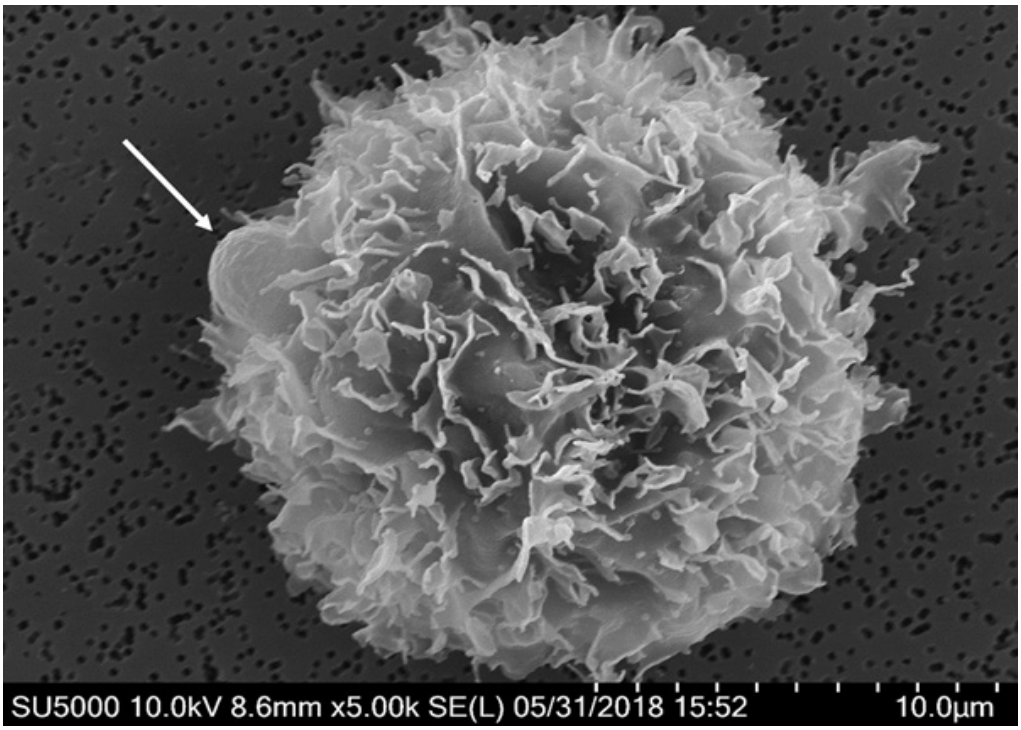

Figure 3. Scanning electron microscopy.

Scanning electron micrograph of a cell phenotypically consistent with an adipose-derived stem cell conjugated to a paramagnetic immunobead (arrow).

Discussion

Similarities in the transplantation and regeneration of cells of the human hematopoietic system and cells of human solid tissues have been long recognized. The first allogeneic hematopoietic stem cell transplant was conducted by Dr. E. Donnall Thomas and reported in the *New England Journal of Medicine* in 1957 [30]. At the Peter Bent Brigham Hospital in Boston, Dr. Thomas was a practicing hematologist and close colleagueand collaborator of Dr. Joseph Murray, a practicing plastic surgeon who had performed the first kidney transplant three years earlier. Both doctors aspired similar passion for transplantation, albeit one of the hematopoietic system and one of solid tissues. For their revolutionary work, they shared the Nobel Prize in Physiology or Medicine in 1990. Those transplantation events set the stage for rapid accrual of scientific research to exploit the therapeutic potential of HSCs from bone marrow and MSCs from solid tissues.

In hematopoietic cell transplantation, while several types of cells may be transplanted, HSCs are the necessary constituents [31]. HSCs are multipotent cells that self-renew and regenerate most, if not all, of the cellular populations found in blood [5,16,32]. Similarly, MSCs also self-renew and are multipotent, with the ability to regenerate solid tissues such as fat, bone, cartilage, nerve, and muscle [33-36]. As both HSCs and MSCs reside in the bone marrow, MSCs support hematopoiesis and associated connective tissue [37]. While bone marrow remains a reliable source of MSCs, solid mesenchymal tissues contain greater quantities of MSCs than marrow [13]. Accordingly, using solid donor mesenchymal tissues for MSC transplantation and regeneration may intend safety, economic, and logistic benefits.

Since their development almost four decades ago, paramagnetic microbeads (or microspheres) have shown great utility in cell separation assays [23,24,26]. In 2017, the Food & Drug Administration approved the first cell therapy for leukemia which uses paramagnetic microspheres to isolate T cells [38]. The T cells were subsequently culture expanded and reinfused. Paramagnetic microspheres, with their polymer shell covering a uniform-sized ferrous core, allow attachment of bioreactive molecules which aid in separation of selected cellular subpopulations. In the current study, primary antibody and secondary ASC-selective antibodies were bound to paramagnetic microspheres which were previously coated with protein-G affinity matrix. A rabbit anti-mouse IgG antibody was applied first. The secondary antibodies were mouse anti-human IgG antibodies of specific clusters of differentiation. These secondary antibodies, CD44, CD73, CD90, and CD105, correspond to known antibod-

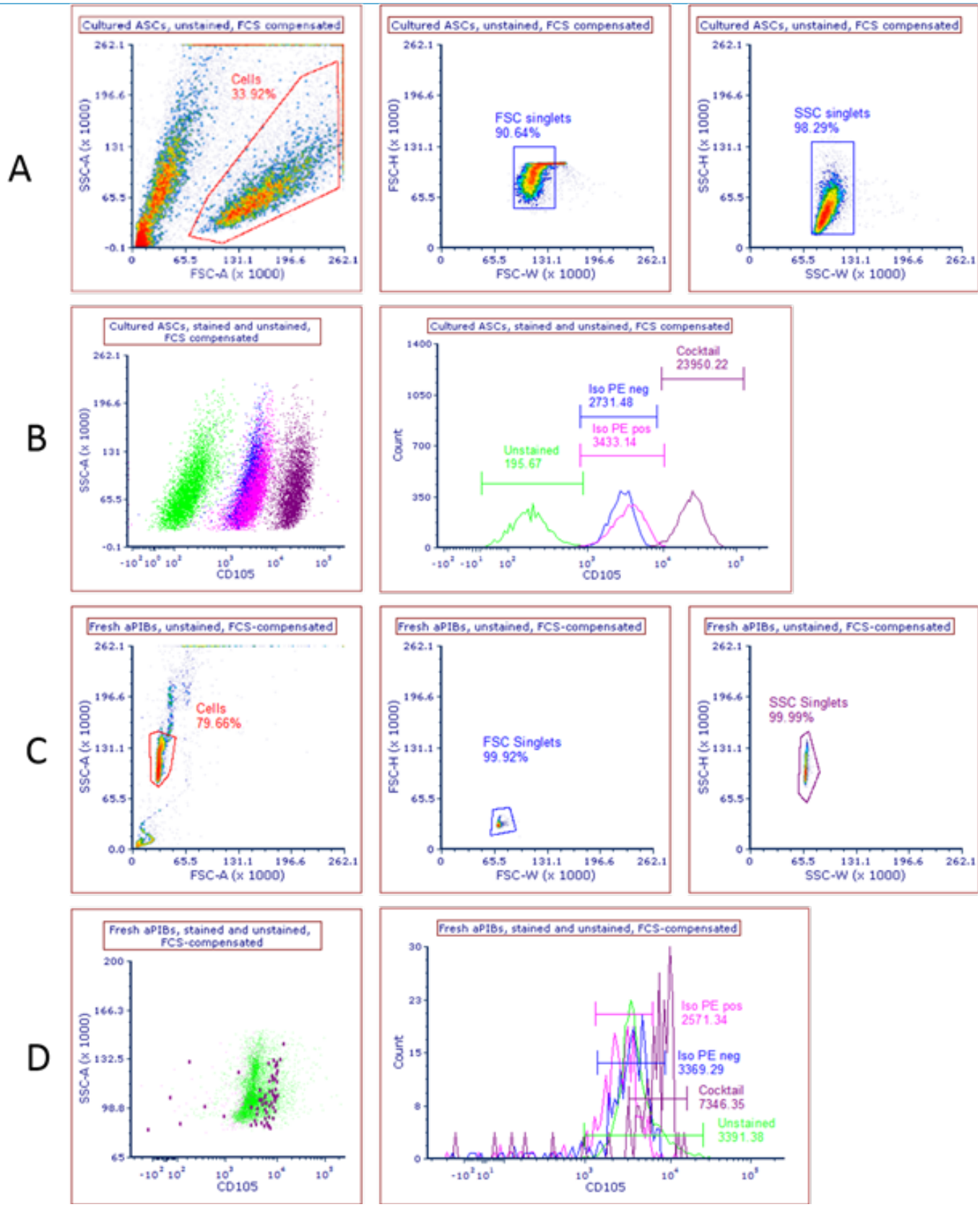

Figure 4. Immunophenotyping of primary adipose-derived cells (ascs) isolated with paramagnetic immunobeads (pibs).
Row A: Scatter plots of cultured ASCs displaying gating to singlets.
Row B: Scatter plot and histogram of cultured ASCs displaying positive CD105 (PerCP-Cy™5.5-CD105) as part of the "Cocktail."
Row C: Scatter plot of freshly isolated ASC-PIB conjugates (aPIBs) with gating to singlets.
Row D: Scatter plot and histogram displaying positive CD105 (PerCP-Cy™5.5-CD105) as part of the "Cocktail." While FITC-CD90 also displayed similar positivity, APC-CD73 and PE-CD44 were not clearly appreciated due to the auto-fluorescence of the PIBs.

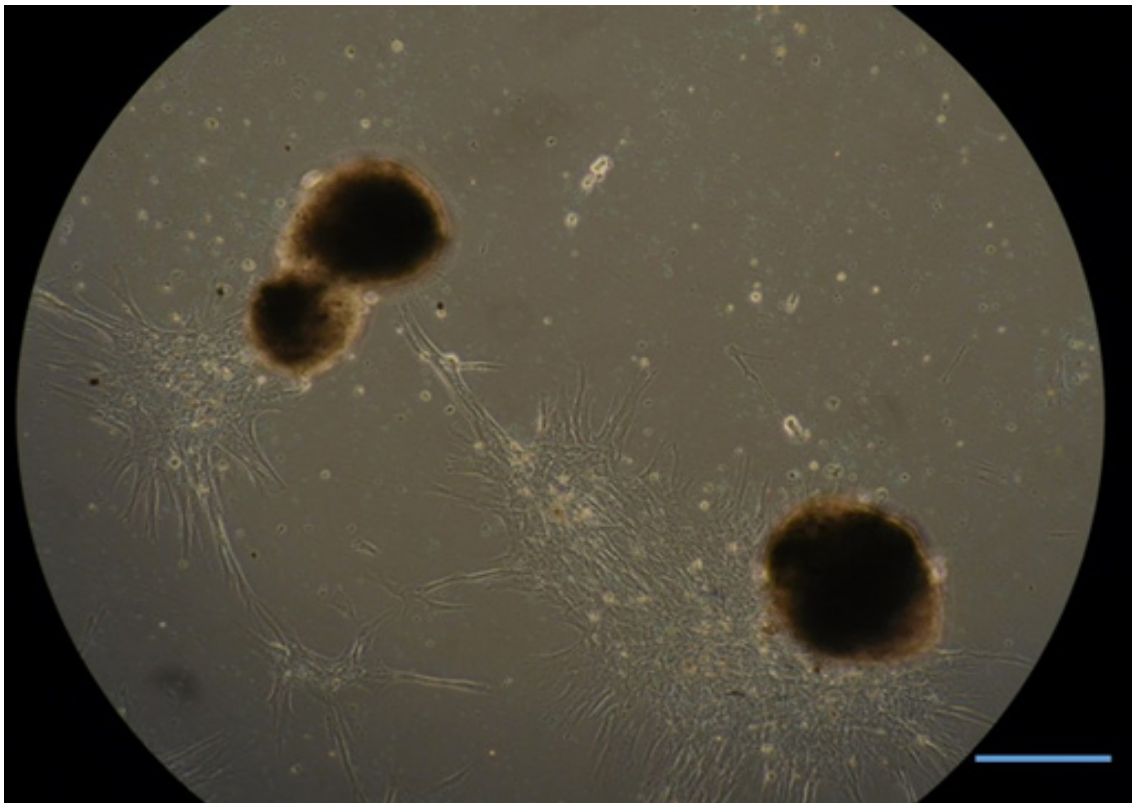

Figure 5. Culture morphology.

Bright-field micrograph of flat plate culture morphology of adipose-derived stem cells precipitated from lipoaspirate with paramagnetic immunobeads (day 14).
Well-organized spheres have developed as well as large colonies. Most of the paramagnetic immunobeads have become spontaneously unconjugated. (10x, measurement bar is 250 μm).

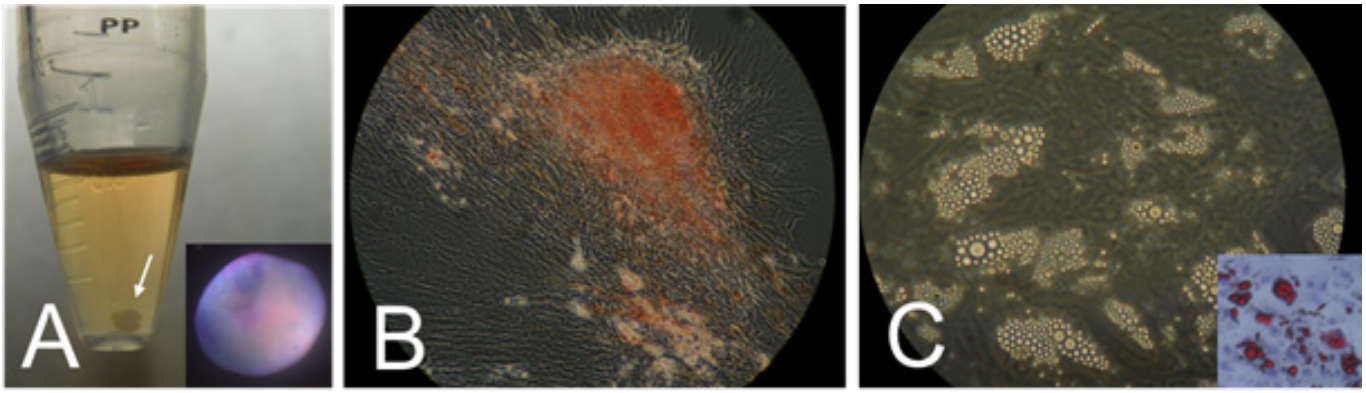

Figure 6. Tri-lineage differentiation.

Tri-lineage differentiation of adipose-derived stem cells precipitated with paramagnetic immunobeads.
Panel A: CHONDROBLAST DIFFERENTIATION: Gross chondrosphere (at white arrow) with representative indirect micrograph illustrating a sulfated proteoglycan sphere (inset) stained with Alcian Blue & Nuclear Fast Red, consistent for chondroblasts. Sphere diameter about 3mm.
Panel B: OSTEOBLAST DIFFERENTIATION:Phase contrast 20x micrograph illustrating alkaline phosphatase staining with Alizarin Red, consistent for osteoblasts.
Panel C: ADIPOCYTE DIFFERENTIATION: Phase contrast 10x micrograph illustrating large lipid filled droplets, consistent for adipocytes (higher power inset with lipid droplet staining by Oil-Red-O).

ies which attach to and define ASCs [39]. While the ASC-specific antibodies may be conjugated directly to the paramagnetic beads, concern for steric hindrance, theoretically reducing cell conjugation, led to this dual layering of IgG antibodies. While ASCs in suspension maintain a spherical shape with extensive undulating surface features [40], termed pseudopodia, we theorized that maximizing separation of the antigen binding sites by the use of selected secondary antibodies would provide greater binding opportunity as well as binding strength as the PIBs situated between the pseudopodia. The greater attachment force would maximally complement the required high magnetic gradient to counteract the significant drag forces within the lipoaspirate. A corresponding neodymium bar magnet was selected for generation of a high magnetic gradient. Additionally, triturating the lipoaspirate (transferring the lipoaspirate between syringes repeatedly) to a fine heterogeneous suspension likely aided the magnetic precipitation of the aPIBs by decreasing magnetic drag (possibly by stripping some ASCs from the stroma thus increasing magnetic cellular velocity).

During this positive selection technique for antibody-mediated enrichment of ASCs, certainly other nucleated cells were isolated as part of the immunoprecipitated cellular population. However, culture expansion of this population selected an apparent single cell population phenotypically consistent with functional ASCs, as defined by morphology, colony development, and trilineage differentiation. Additionally, flow cytometry clearly displayed isolated cells exhibiting the CD90 and CD105 markers, as found on ASCs. Not unexpectedly, the PIBs themselves exhibited intense auto-fluorescence, shadowing the representative fluorescence of the APC marker for CD73 and the PE marker for CD44. Unconjugating the aPIBs will be needed to confirm the presence of these antibodies. However, leaving the aPIBs conjugated for expansion and tri-lineage differentiation did not seem to alter respective ASC function. Follow-on studies will optimize the quality and quantity of the enriched ASCs.

The technique presented in this study may isolate clinically useful quantities of ASCs without culturing, as is typically found with many therapies using BMSCs. While BMSCs certainly can be used in therapy as primary cells, *in vitro* expansion of BMSCs requires days to weeks to reach quantities necessary for maximal efficacy. However, as ASCs are more numerous in solid tissues, a clinically therapeutic quantity of primary ASCs may be isolated and infused at the point-of-care. Additionally, studies have highlighted other related risks and tradeoffs of *in vitro* expansion, to include contamination, influences on proliferating, differentiation and homing potential [41-43], and acquisition of tumorigenic properties [15,44,45]. Such risks would be reduced by the use of primary ASCs.

Conclusions

This study validates that functional ASCs may be isolated from aspirated adipose tissue by paramagnetic enrichment in 20 minutes. As the aspiration of adipose tissue and the subsequent enrichment of ASCs do not require electricity, primary therapeutic ASCs may now be isolated in any point-of-care setting, even in developing countries where access to electricity is difficult if not impossible.

References

1. Lorenz e, uphoff d, reid tr, shelton e (1951) Modification of irradiation injury in mice and guinea pigs by bone marrow injections. J Natl Cancer Inst 12: 197-201.

2. Friedenstein AJ, Gorskaja JF, Kulagina NN (1976) Fibroblast precursors in normal and irradiated mouse hematopoietic organs. Exp Hematol 4: 267-274.

3. Becker aj, mcculloch ea, till je (1963) Cytological demonstration of the clonal nature of spleen colonies derived from transplanted mouse marrow cells. Nature 197: 452-454.

4. TILL JE, mcculloch EA (1961) A direct measurement of the radiation sensitivity of normal mouse bone marrow cells. Radiat Res 14: 213-222.

5. Till je, mcculloch ea, siminovitch l (1964) A stochastic model of stem cell proliferation, based on the growth of spleen colony-forming cells. Proc Natl Acad Sci U S A 51: 29-36.

6. Caplan AI (1991) Mesenchymal stem cells. J Orthop Res 9: 641-650.

7. Pittenger MF, Mackay AM, Beck SC, et al. (1999) Multilineage potential of adult human mesenchymal stem cells. Science 284: 143-147.

8. Zuk PA, Zhu M, Mizuno H, et al. (2001) Multilineage cells from human adipose tissue: Implications for cell-based therapies. Tissue Eng. 7: 211-228.

9. Wagner W, Wein F, Seckinger A, et al. (2005) Comparative characteristics of mesenchymal stem cells from human bone marrow, adipose tissue, and umbilical cord blood. Exp Hematol. 33: 1402-1416.

10. Fraser JK, Wulur I, Alfonso Z, Hedrick MH (2006) Fat tissue: An underappreciated source of stem cells for biotechnology. Trends Biotechnol 24: 150-154.

11. Helder MN, Knippenberg M, Klein-Nulend J, Wuisman PI (2007) Stem cells from adipose tissue allow challenging new concepts for regenerative medicine. Tissue Eng 13:1799-1808.

12. Strem BM, Hicok KC, Zhu M, et al. (2005) Multipotential differentiation of adipose tissue-derived stem cells. Keio J Med 54:132-141.

13. Sakaguchi Y, Sekiya I, Yagishita K, Muneta T (2005) Comparison of human stem cells derived from various mesenchymal tissues: Superiority of synovium as a cell source. Arthritis Rheum 52: 2521-2529.

14. Morizono K, De Ugarte DA, Zhu M, et al. (2003) Multilineage cells from adipose tissue as gene delivery vehicles. Hum Gene Ther 14: 59-66.

15. Kim HJ, Park JS (2017) Usage of human mesenchymal stem cells in cell-based therapy: Advantages and disadvantages. Dev Reprod 21:1-10.

16.NIH.Regenerative medicine. https://stemcells.nih.gov/info/Regenerative_Medicine/2006Chapter2.htm. Updated 2006. Accessed 01/11, 2019.

17. NIH. Stem cells. https://stemcells.nih.gov/info/2001report/chapter5.htm. Updated 2001. Accessed 01/27, 2019.

18. Zhu B, Murthy SK (2013) Stem cell separation technologies. Curr Opin Chem Eng 2: 3-7.

19. Gothard D, Tare RS, Mitchell PD, Dawson JI, Oreffo RO (2011) In search of the skeletal stem cell: Isolation and separation strategies at the macro/micro scale for skeletal regeneration. Lab Chip. 11: 1206-1220.

20. Bauer J (1999) Advances in cell separation: Recent developments in counterflow centrifugal elutriation and continuous flow cell separation. J Chromatogr B Biomed Sci Appl 722: 55-69.

21. Thiel A, Scheffold A, Radbruch A (1998) Immunomagnetic cell sorting--pushing the limits. Immunotechnology 4: 89-96.

22. Putnam DD, Namasivayam V, Burns MA (2003) Cell affinity separations using magnetically stabilized fluidized beds: Erythrocyte subpopulation fractionation utilizing a lectin-magnetite support. Biotechnol Bioeng 81: 650-665.

23. Ugelstad J, Mork P, Kaggerud K, Ellingsen T, Berge A (1980) Swelling of oligomer-polymer particles. new methods of preparation. Advances in colloid and interface science 13: 101-140.

24. Ugelstad J, Stenstad P, Kilaas L, et al. (1993) Monodisperse magnetic polymer particles. new biochemical and biomedical applications. Blood Purif 11: 349-369.

25. Safarik I, Safarikova M (2004) Magnetic techniques for the isolation and purification of proteins and peptides. Biomagn Res Technol 2: 7-044X-2-7.

26. Neurauter AA, Bonyhadi M, Lien E, et al. (2007) Cell isolation and expansion using dynabeads. Adv Biochem Eng Biotechnol 106: 41-73.

27. Safarik I, Safarikova M (1999) Use of magnetic techniques for the isolation of cells. J Chromatogr B Biomed Sci Appl 722: 33-53.

28. Wognum AW, Eaves AC, Thomas TE (2003) Identification and isolation of hematopoietic stem cells. Arch Med Res 34: 461-475.

29. Cherry EM, Maxim PG, Eaton JK (2010) Particle size, magnetic field, and blood velocity effects on particle retention in magnetic drug targeting. Med Phys 37:175-182.

30. Thomas Ed, Lochte Hl, Jr, Lu Wc, Ferrebee Jw (1957) Intravenous infusion of bone marrow in patients receiving radiation and chemotherapy. N Engl J Med 257: 491-496

31. Weissman IL, Shizuru JA (2008) The origins of the identification and isolation of hematopoietic stem cells, and their capability to induce donor-specific transplantation tolerance and treat autoimmune diseases. Blood 112: 3543-3553.

32. Spangrude GJ, Heimfeld S, Weissman IL (1998) Purification and characterization of mouse hematopoietic stem cells. Science 241: 58-62.

33. Brown SA, Levi B, Lequeux C, Wong VW, Mojallal A, Longaker MT (2010) Basic science review on adipose tissue for clinicians. Plast Reconstr Surg. 126: 1936-1946.

34. De Francesco F, Ricci G, D'Andrea F, Nicoletti GF, Ferraro GA (2015) Human adipose stem cells: From bench to bedside. Tissue Eng Part B Rev 21:572-584.

35. Zuk PA, Zhu M, Mizuno H, et al. (2001) Multilineage cells from human adipose tissue: Implications for cell-based therapies. Tissue Eng. 7:211-228.

36. Zuk PA, Zhu M, Ashjian P, et al. (2002) Human adipose tissue is a source of multipotent stem cells. Mol Biol Cell. 13: 4279-4295.

37. NIH. Stem cells. https://stemcells.nih.gov/info/basics/4.htm. Updated 2016. Accessed 02/04, 2019.

38. PR Newswire. First FDA-approved cell therapy for leukemia utilizes thermo fisher scientific's CTS dynabeads technology. https://www.prnewswire.com/news-releases/first-fda-approved-cell-therapy-for-leukemia-utilizes-thermo-fisher-scientifics-cts-dynabeads-technology-300511732.html. Updated August 30, 2017. Accessed March 26, 2018.

39. Bourin P, Bunnell BA, Casteilla L, et al. (2013) Stromal cells from the adipose tissue-derived stromal vascular fraction and culture expanded adipose tissue-derived stromal/stem cells: A joint statement of the international federation for adipose therapeutics and science (IFATS) and the international society for cellular therapy (ISCT). Cytotherapy 15: 641-648.

40. Raimondo S, Penna C, Pagliaro P, Geuna S (2006) Morphological characterization of GFP stably transfected adult mesenchymal bone marrow stem cells. J Anat 208 :3-12.

41. Bonab MM, Alimoghaddam K, Talebian F, Ghaffari SH, Ghavamzadeh A, Nikbin B (2006) Aging of mesenchymal stem cell in vitro. BMC Cell Biol 7:14-2121-7-14.

42. Chachques JC, Herreros J, Trainini J, et al. (2004) Autologous human serum for cell culture avoids the implantation of cardioverter-defibrillators in cellular cardiomyoplasty. Int J Cardiol 95 Suppl 1:S29-33.

43. Rombouts WJ, Ploemacher RE (2003) Primary murine MSC show highly efficient homing to the bone marrow but lose homing ability following culture. Leukemia 17:160-170.

44. Miura M, Miura Y, Padilla-Nash HM, et al. (2006) Accumulated chromosomal instability in murine bone marrow mesenchymal stem cells leads to malignant transformation. Stem Cells 24:1095-1103.

45. Tolar J, Nauta AJ, Osborn MJ, et al. (2007) Sarcoma derived from cultured mesenchymal stem cells. Stem Cells 25: 371-379.